Composite Structures 161 (2017) 15–22

Contents lists available at ScienceDirect

Composite Structures

journal homepage: www.elsevier.com/locate/compstruct

Improvement of the in-plane crushing response of CFRP sandwich panels by through-thickness reinforcements

L.G. Blok [a,b], J. Kratz [c,*], D. Lukaszewicz [b], S. Hesse [b], C. Ward [c], C. Kassapoglou [a]

[a] Faculty of Aerospace Engineering, Delft University of Technology, Kluyverweg 1, 2629 HS Delft, The Netherlands
[b] BMW Group, Department, Research and Innovation Centre, Knorrstrasse 147, 80788 Munich, Germany
[c] ACCIS, University of Bristol, Queen's Building, University Walk, BS8 1TR Bristol, United Kingdom

ARTICLE INFO

Article history:
Received 1 August 2016
Revised 10 November 2016
Accepted 11 November 2016
Available online 12 November 2016

Keywords:
Energy absorption
Impact behaviour
Through-thickness reinforcement
Composite sandwich panel

ABSTRACT

Fibre reinforced plastic (FRP) composite materials can provide superior specific energy absorption performance over conventional metallic structures if crush stability can be maintained during the impact event. The core in sandwich structures helps to stabilise the crush front by preventing global buckling, but delamination remains a barrier to optimal crushing performance. In this work, the in-plane crushing response of sandwich structures was improved by adding through-thickness reinforcement in the form of aramid fibre tufts. The effect of tufting different sandwich cores and facesheet orientations was investigated in both static and dynamic crushing modes. A drop-tower test rig was used to crush panels in realistic automotive crash conditions and a high-speed camera captured the crushing mechanisms. The through-thickness reinforcement improved the facesheet to core adhesion, resulting in a more localised and stable fracture of the facesheets. Tufting improved the specific energy absorption (SEA) from 11.5 kJ/kg to 20.5 kJ/kg and the crush force efficiency (CFE) from 0.22 to 0.55.

1. Introduction

Fibre reinforced plastic (FRP) composite materials are gaining interest from car manufacturers for many reasons. In addition to higher stiffness, fibre reinforced composites can provide superior energy absorption performance over conventional metallic structures, when compared by weight [1]. The use of composite materials as energy absorbers, however, is still limited as they crush in a more unstable manner than their metallic counterparts [2]. In a real-world crash situation, load scenarios are not well defined and this restricts the design of energy dissipating composite structures to beams and profiles at the moment [3]. Composite sandwich structures may provide a more stable crushing mechanism for fibre reinforced materials, enabling new vehicles with flat, shell-line structures capable of absorbing energy in multiple load paths in a crash event.

FRP composite materials typically crush in a brittle manner, which can result in unstable catastrophic failure, but if properly controlled, stable progressive end-crushing is possible. Progressive crushing is characterised by a localised zone of micro fracturing of the composite material consisting of splaying/lamina bending and fragmentation/fibre fracture [1,4,5]. Several studies have investigated the change in energy absorption of FRP crush tubes using interlaminar toughening techniques [6], surface treatments [7], different matrix properties [8,9] and different fibre orientations [10]. These studies showed that higher interlaminar properties lead to less splaying/lamina bending, resulting in higher energy absorption.

Most studies investigating impact events to sandwich structures have focused on the out-of-plane impact loading [10,11], commonly related to bird strike in aerospace applications. The in-plane (or edgewise) crushing of sandwich structures has received less attention in the literature, but becomes more relevant for automotive crashworthiness. The study by Mamalis et al. [12] reported three different collapse modes for edgewise compression of composite sandwich structures: unstable sandwich column buckling (Mode 1); unstable sandwich disintegration by facesheet/core disbonding (Mode 2); and progressive end crushing of the sandwich (Mode 3). They identified that the mechanical properties of the core have a large effect on the failure mode, as the core stabilises the facesheets during crushing and prevents sandwich disintegration [11,12].

Introducing a foam core may stabilise the crushing of the fibre layers, but this adds another interface to the structure which can disbond, resulting in unstable collapse. Stapleton and Adams [13]

* Corresponding author.
E-mail address: james.kratz@bristol.ac.uk (J. Kratz).

http://dx.doi.org/10.1016/j.compstruct.2016.11.034
0263-8223/

investigated the effect of crush initiators to promote stable crushing of sandwich panels. They propose that a stable crushing mode depends on the strength and stiffness of the core, the composite facesheet, and the strength of the facesheet/core interface [13]. However, increasing the stiffness and strength of the facesheets does not necessarily improve the energy absorption as facesheet buckling failure may occur, reducing the energy absorbed during the impact event. More recently, they reported on structural enhancements (end-bevel, stitching and core webbing) to improve the energy absorption [14]. Their findings suggest that stable sandwich crushing may be realised by improving the facesheet/core interface.

To successfully implement the superior energy absorption of composites, a stable and predictable crushing platform is required. In this work, an improvement in crushing response is obtained by through-thickness reinforcements of the facesheets to the core using aramid fibre tufts. This effectively creates a three-dimensional composite structure which has been proposed to improve the impact resistance [15,16]. The advantage of the tufting technique is that it only requires one-sided access to the preform. These tufts strengthen the interface between the facesheet and the core and prevent premature facesheet separation [17,18]. At the same time, the tufts prevent the facesheet plies from delaminating from eachother, further increasing the energy absorbed during the impact event.

Static and dynamic edgewise compression tests were carried-out on eight different panel configurations to identify whether core type and facesheet fibre orientation influence the energy absorbing characteristics. A customised drop-tower test-rig was developed to allow facesheet/core failure, meanwhile a high speed camera was used to record the crushing front. The different crushing mechanisms offer detailed understanding of the failure progression in through-thickness reinforced sandwich structures subjected to edgewise loading.

2. Methodology

2.1. Materials and manufacturing

Sandwich specimens were manufactured using two common foam cores types: *Rohacell 110 IG-F a* polymethacrylimide (PMI) and *Airex C70.90 a* polyvinylchloride (PVC), both 10 mm thick. The main difference between the two foam cores is the maximum strain to failure of 3% versus 23%, as shown in Table 1. The facesheets were made from uniaxial carbon fibre non-crimp fabric (NCF) from SGL automotive with 50 K tows, and a 310 g/m^2 areal weight. The strength and modulus of the fibres according to manufacturer specifications is 4 GPa and 240 GPa, respectively [19].

Hand lay-up was used to preform the sandwich panels, after which a tkt 20 Kevlar® thread (from Somac threads UK) was tufted through the preformed sandwich in a 6 mm × 6 mm square pattern using a KSL tufting head mounted to a Kuka robotic arm at the UK National Composites Centre [17]. A vacuum infusion process was used to saturate the dry perform with RIMR 935/936 resin system from Momentive Speciality Chemicals. The plates were infused at 40 °C and then cured at 90 °C for 2 h under −98.2 kPa (gauge) vaccum pressure. Specimens were waterjet cut from the cured plates and no further machining steps were carried out. Of note, the tufting needle created a void space in the foam core during thread insertion which was then filled during infusion resulting in a resin column around the Kevlar thread, as shown in Fig. 1, and the tufted specimens were on average 28% heavier than the untufted control specimens.

Four different lay-ups were used for the facesheet skins; [0/90/0], $[0/90/0]_s$, [−45/0/45] and $[-45/0/45]_s$, yielding eight different sandwich configurations as summarised in Table 2. The thickness of the facesheets was 1.2 mm for the three ply configurations and 2.3 mm for the six ply configurations. A monolithic traveler laminate was tested for fibre volume fraction by acid digestion and a value of 54.5% was measured with a void volume fraction of 1.9%.

2.2. Test fixture

Most studies investigating the in-plane crushing response of sandwich panels use a fixed specimen and a moving impactor [11,13,14]. In this study, the specimen was mounted to the moving hammer in a drop-tower rig and crushed into a fixed plate, as shown in Fig. 2. The specimen freely falls in between four alignment guides, as in shown in Fig. 3. The advantage of the test set-up used here is that specimen rotation/bending is suppressed without constraining disbonding or delamination over its length. Interface failure between the core and facesheet was recorded at the crush front using a high speed camera.

The test specimen dimensions for the static and dynamic tests are shown in Fig. 4. Static tests were smaller as they were carried out for initial screening of the sandwich panels to determine the impact energy for the dynamic tests. Both specimens included a 14° bevel to promote stable progressive crushing as demonstrated by Velecela et al. [22], as shown in Fig. 4. For each sandwich configuration, three static tests and three dynamics tests were performed.

2.3. Static testing

The static tests were conducted using a hydraulic press as shown in Fig. 5. The test was carried out at a constant displacement rate of 330 mm/min. The displacement and force were directly measured, which could then be used to determine relevant crushing properties such as maximum force, average force and energy absorption.

Table 1
Mechanical properties polymer foams as supplied by manufacturer [20,21].

	Airex C70.90	Rohacell 110 IG-F
Density [kg/m^3]	100	110
Compressive strength [MPa]	2.0	3.0
Compressive modulus [MPa]	130	160
Shear modulus [MPa]	40	50
Maximum strain [%]	23	3

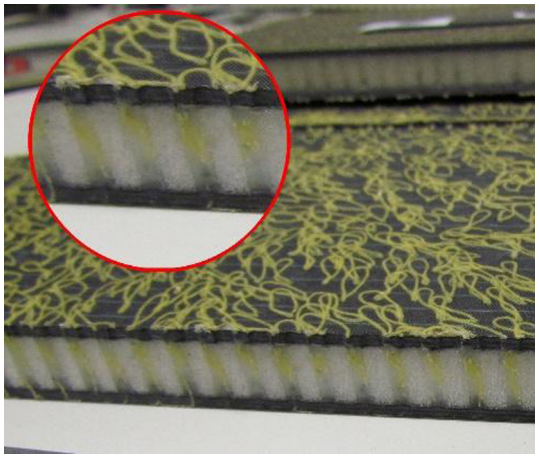

Fig. 1. Example of tufted sandwich specimen showing resin columns around Kevlar tufts (inset).

Table 2
Sandwich configurations for static and dynamic testing.

Facesheet material	Non-crimp fabric
Facesheet lay-ups	[0/90/0], $[0/90/0]_s$, [−45/0/45] and $[-45/0/45]_s$
Core materials	Airex C70.90 and Rohacell 110 IG-F
Through-thickness reinforcement	With and without Kevlar® tufts.

2.4. Dynamic testing

Dynamic testing was carried out by mounting the sandwich specimen under a drop hammer and dropping the entire assembly onto the crush plate, as shown in Fig. 2. The drop height was set to have an impact speed v_{imp} of 8.6 m/s. A mass m_{imp} was added to the drop hammer to change the impact energy E_{imp}. The impact energy was adjusted using the energy absorbed from the static test measurements in order to crush the specimen without colliding the drop hammer into the test fixture.

Two accelerometers recorded the acceleration of the drop-hammer during specimen crushing. The raw accelerometer data was filtered to remove any high frequency oscillation according to the SAE J211 guidelines for impact testing [23]. A CFC 180 filter has been used which is the recommended filter to be used for further integration of the acceleration data to obtain velocity and distance.

The crushing force was determined from the filtered acceleration data a_{acc} using Eq. (1), where m_{imp} is the mass of the drop hammer. The crushing distance was also determined from the filtered acceleration data, by integrating it twice according to Eqs. (2) and (3), where v_{imp} was the initial velocity, s was the distance travelled, and t was the crush time. A representative section of crushing was extracted from each force-displacement curve up to a displacement $s = 75$ mm to obtain a common basis for all sandwich panels.

$$F = m_{imp} a_{acc} \tag{1}$$

$$v(t) = v_{imp} - \int_0^t a_{acc}\,dt \tag{2}$$

$$s(t) = \int_0^t v\,dt \tag{3}$$

2.5. Crushing properties

Two force-displacement curves for the dynamic and static tests are shown in Fig. 6 to illustrate the typical crushing response measured during testing. The force-displacement curve of the dynamic test (Fig. 6a) shows less detail than that of the static test (Fig. 6b). The dynamic data has been filtered to remove high frequency noise. The use of filtering prevented visual correlation between the local failure mechanisms and force recorded during crushing. The crushing performance of each sandwich configuration was compared using the global crushing properties indicated in Fig. 6. The crushed mass $m_{crushed}$ needed to determine the specific energy absorption was derived from the crushing distance and the density of the specimen, and the energy absorbed $E_{absorbed}$ was calculated by integrating the force-displacement graph. The following parameters were identified from each test:

- Maximum recorded force during crushing F_{max}.
- Average crushing force during entire crushing event F_{avg}.
- Crush force efficiency (CFE = F_{avg}/F_{max}).
- Specific energy absorption (SEA = $E_{absorbed}/m_{crushed}$).

3. Results and discussion

3.1. Maximum force and average crushing force

The maximum force supported by the sandwich specimens occurs at the early stages of loading, as shown in Fig. 6. The sandwich structure elastically compresses under the applied load until damage is initiated at the trigger. The maximum crushing force of the different configurations (three specimens per configuration) is shown in Fig. 7. An overall increasing trend was observed in the maximum force by adding the through-thickness reinforcement. The tufts increase the load required to initiate failure of the facesheet-core interface. One exception was observed in the C70.90 $[0/90/0]_s$ sandwich system, where a small decrease in maximum force was recorded. This configuration has relatively stiff facesheets, due to the predominantly 0° ply orientation and number of plies, supported by a ductile foam core. In contrast, the 110 IG-F [0/90/0] sandwich panels showed the highest increase in maximum force, due to the thinner facesheets and brittle foam core providing less support during crushing.

Once damage was initiated in the sandwich specimens, the load supported decreases, as shown in Fig. 6. At this point in the impact event is where the through-thickness reinforcement is truly advan-

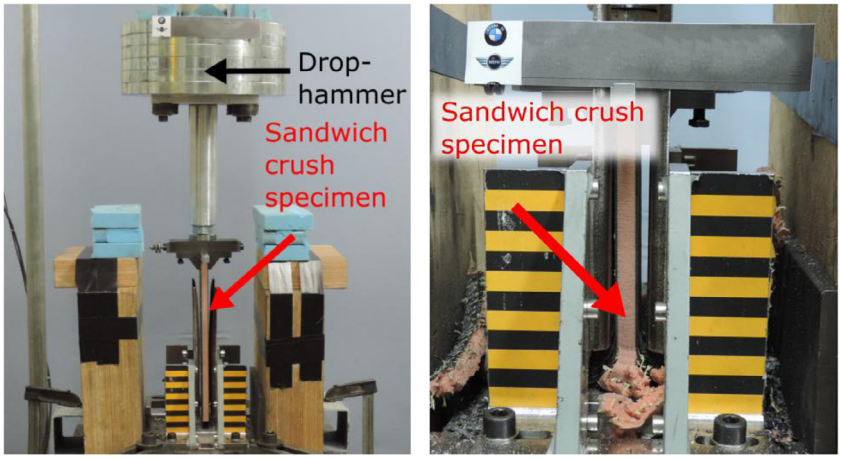

Fig. 2. Test set-up showing sandwich crush specimen before and after crushing in test fixture.

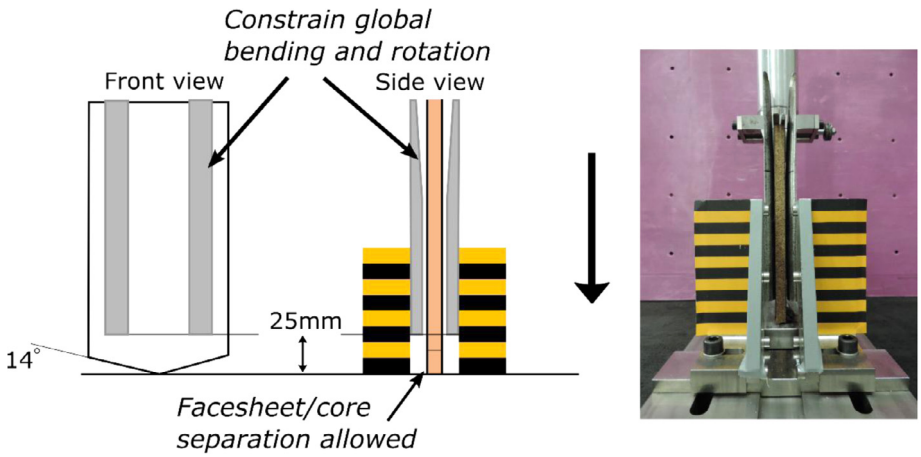

Fig. 3. Detail of test fixture showing sandwich specimen and four alignment guide rods and impact plate.

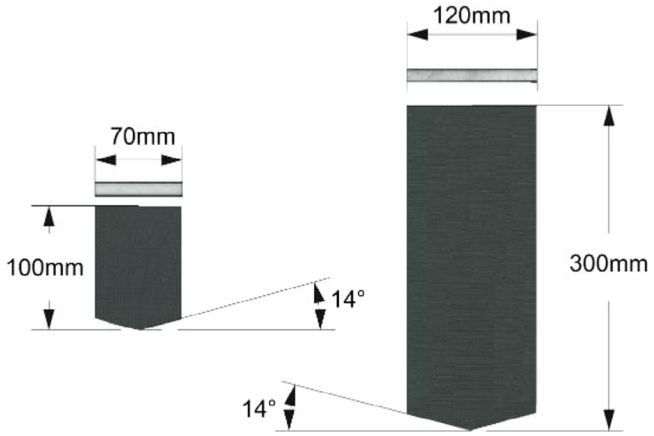

Fig. 4. Dimensions of the test specimens for static (left) and dynamic (right) tests.

tageous. The average crushing force in all sandwich configurations was improved by tufting, as shown in Fig. 8. In all facesheet lay-ups, the brittle 110 IG-F sandwiches structures shows greater improvement due to tufting compared to the more ductile Airex C70.90 sandwiches. The average crushing force does not take into account the increase in sandwich mass due to tufting, as a result, the SEA and CFE analysis in the following section offers a more direct comparison to the crashworthiness benefits of tufting sandwich structures.

3.2. Specific energy absorption and crush force efficiency

Tufting clearly improved the specific energy absorption (SEA) of all sandwich panels under dynamic and static crushing, as shown in Fig. 9. The average increase in SEA during dynamic crushing for the Rohacell 110 IG-F sandwiches was 117%, and for the Airex C70.90 sandwiches the average increase was 52%. Furthermore, the SEA during dynamic crushing is consistently 60% lower than in static test conditions. This difference may be attributed to the strain-rate dependency of the material. During dynamic impact, the strain-rate sensitivity of the material system becomes important, which is more dominant for the matrix response and friction forces [24]. In the dynamic tests, the predominant failure mode was delamination which is described in Section 3.3.

Fig. 9 also shows that the SEA of untufted C70.90 sandwich panels generally exceeded that of the untufted 110 IG-F sandwiches. When the tufted sandwiches are compared, the 110 IG-F sandwiches show a higher SEA than the C70.90 sandwiches. The 110 IG-F sandwich panels showed a larger relative improvement by tufting than similar C70.90 sandwiches. The crushing response of the untufted sandwich panels tested in this paper are in agreement to those reported by Mamalis et al. [11], where foam cores with higher ductility better stabilise the facesheets during crushing.

The different facesheet lay-ups show how the SEA changes with thicker and/or stiffer facesheets. For untufted sandwiches under dynamic crushing, thicker facesheets ($[0/90/0]_s$ and $[-45/0/45]_s$) showed a higher SEA than similar thinner facesheets ([0/90/0] and [−45/0/45]). For the tufted sandwiches, however, the thickness

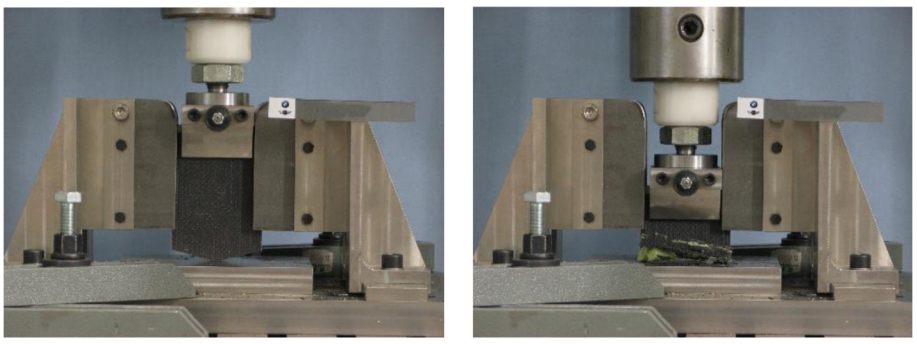

Fig. 5. Sandwich specimens in a hydraulic press (a) before and (b) after static testing.

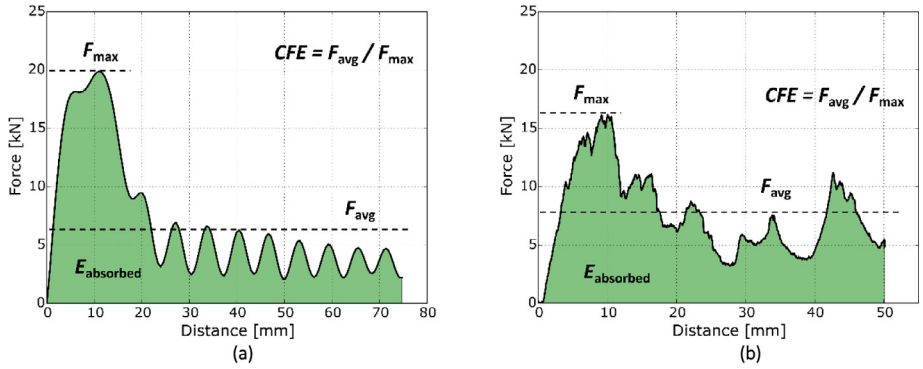

Fig. 6. Force-displacement response of C70.90 [0/90/0] sandwich in (a) dynamic and (b) static crushing.

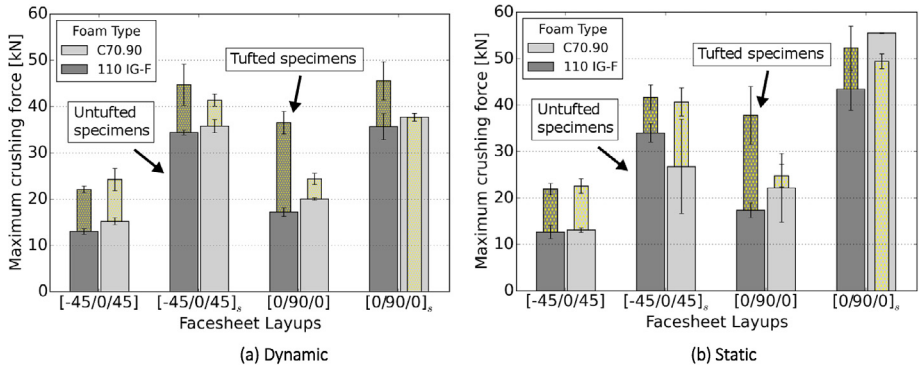

Fig. 7. Maximum crushing force during (a) dynamic and (b) static testing.

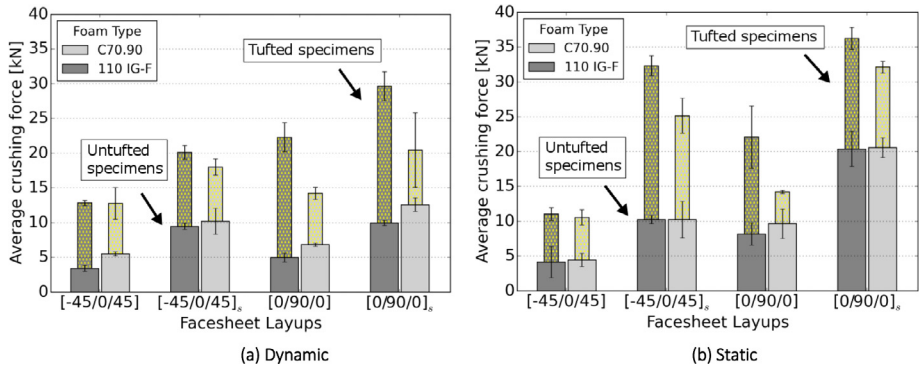

Fig. 8. Average crushing force during (a) dynamic and (b) static testing.

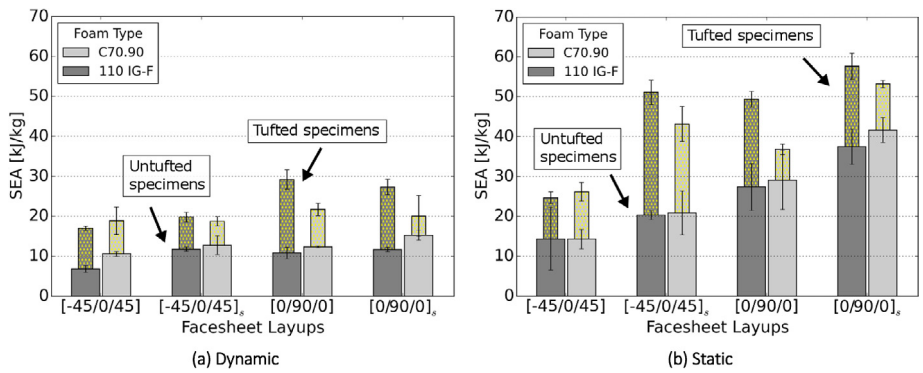

Fig. 9. Specific energy absorption of sandwich specimens in (a) dynamic and (b) static crushing.

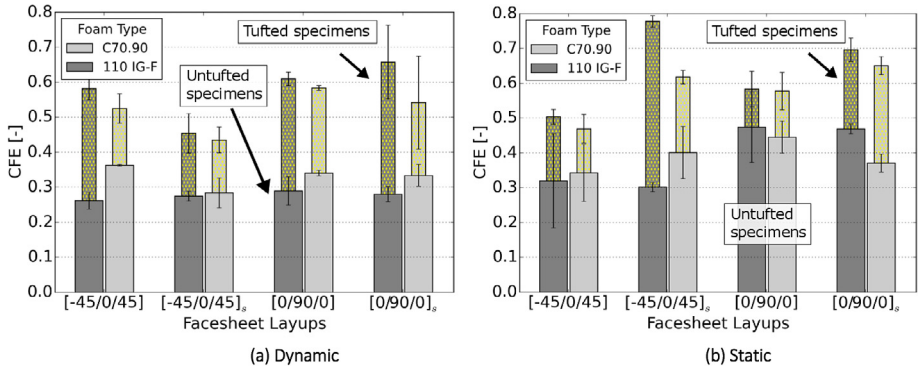

Fig. 10. Crush force efficiency (F_{avg}/F_{max}) during (a) dynamic and (b) static testing.

Table 3
Observed Crushing Mechanisms of Sandwich Panels.

	Non Tufted	Tufted
Brittle Rohacell 110 IG-F	Dominated by separation of the facesheet from the core, and bending of the separated facesheet	Localized splaying and fracture of facesheet (Mode 3 progressive crushing)
Ductile Airex C70.90	Dominated by delaminations in the facesheet, core build-up and bending of the delaminated facesheet	Localized splaying and fracture of facesheet (Mode 3 progressive crushing)

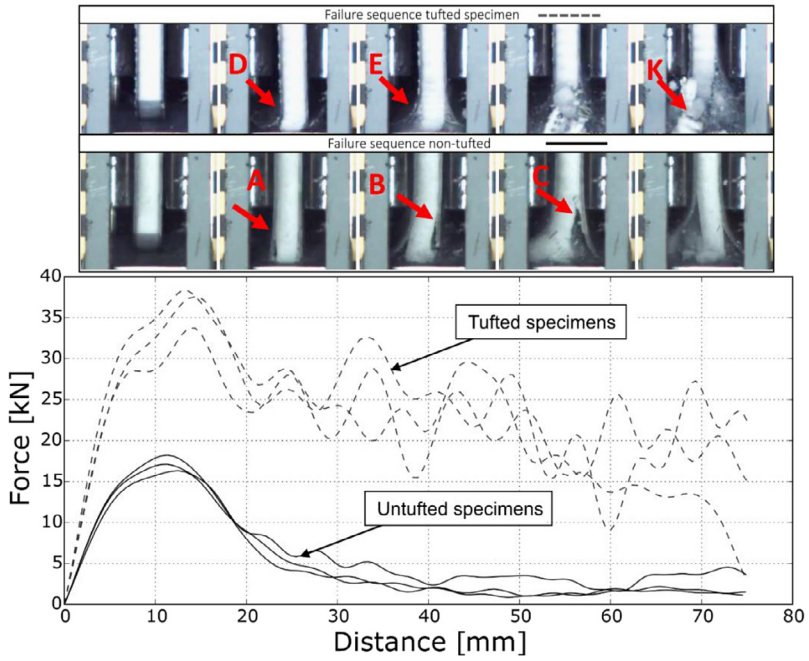

Fig. 11. Comparison of force-displacement curves of Rohacell 110 IG-F [0/90/0] sandwiches (3× tufted & 3× non-tufted), with typical failure sequence.

of the facesheets seem to have little effect on the SEA during dynamic crushing.

For each sandwich configuration, three specimens were tested. The coefficient of variation in SEA was 9% on average over all dynamic test specimens and 12.9% for the static test specimens. During crushing, different failures occur progressively over a representative distance, which may reduce the global error as it is the average of all fracture.

Fig. 10 shows the crush force efficiency (CFE = F_{avg}/F_{max}) during static and dynamic crushing for the different sandwich panels. The average improvement by tufting in dynamic crushing of the 110 IG-F sandwiches was +100% (+225% in static crushing) and for the C70.90 sandwiches +58% (+214% in static crushing). This indicates that tufting increased the energy absorption by having a higher sustained crushing force compared to the initial peak load.

3.3. Crushing mechanisms

A comparison of the crushing mechanisms for the different sandwich panels is shown in Table 3. No unstable sandwich column buckling was observed in these tests, confirming that the trigger was an effective initiator of facesheet/core disbonding and progressive end crushing of the sandwich. A difference in crushing response was observed in the untufted panels, where the core duc-

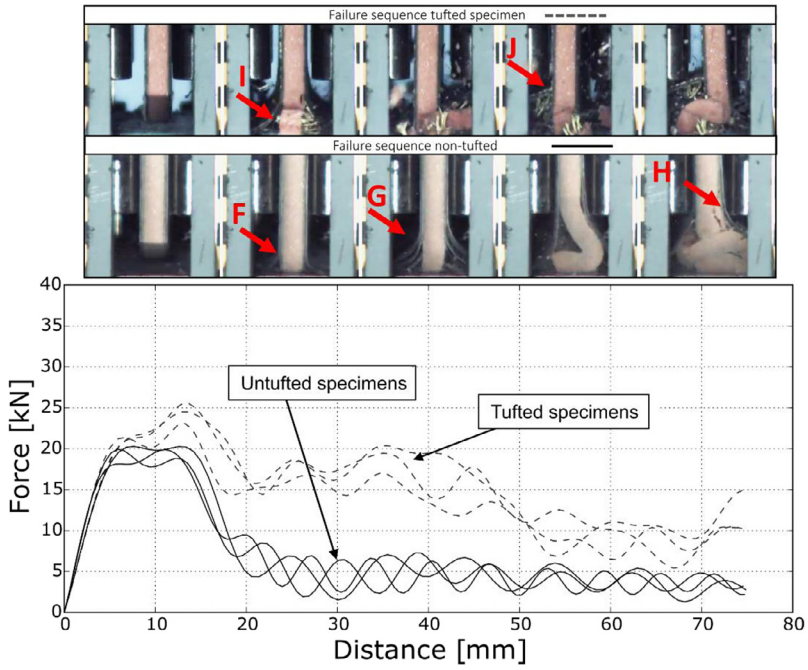

Fig. 12. Comparison of force-displacement curves of Airex C70.90 [0/90/0] sandwiches (3× tufted and 3× non-tufted) with typical failure sequence.

tility influenced facesheet core separation as reported by Mamalis et al. [11]. The crushing response was improved for both ductile and brittle cores by tufting, which led to more localised progressive end crushing in both instances.

The main crushing mechanisms observed during edgewise loading and the corresponding force-displacement graphs of the 110 IG-F [0/90/0] and C70.90 [0/90/0] sandwiches are shown in Figs. 11 and 12. Facesheet/core interfacial failure was the dominant failure mechanism in the untufted 110 IG-F sandwich panels, and is clearly visible from the start of crushing, as shown in Fig. 10 (see arrows A, B and C). The facesheet/core disbonding remained the only failure mode present throughout crushing. When tufting was introduced to the sandwich, the facesheets remained attached to the core and bent through a small radius (arrows D and E) before the Mode 3 fracture processes started.

The failure of the untufted C70.90 [0/90/0] specimen was initiated by delaminations in the facesheets (arrows F and G), with subsequent bending of the facesheets (arrow H). In contrast untufted 110 IG-F sandwich panels, little fracture of the facesheet or disbonding of the facesheet/core was observed. Instead, core debris built up on the crush plate. For the tufted C70.90 specimens, no delaminations within the facesheet were observed. Although some facesheet/core disbonding failure was observed (arrow I), clearly more facesheet fracture (arrow J) was present together with crushing of the core material.

Overall, the untufted C70.90 [0/90/0] specimens had a higher energy absorption than the untufted 110 IG-F [0/90/0] specimens. This was attributed to the extra energy required to delaminate the plies within the C70.90 specimen facesheets, whereas less energy was absorbed by the untufted 110 IG-F specimens because the facesheets simply disbonded from the core and subsequently bent.

Adding the tufts to the sandwich panels introduced a facesheet fracture mechanism to both the C70.90 and the 110 IG-F specimens. The tufted 110 IG-F specimens showed more fracture and fragmenting of the foam core (arrow K) compared to tufted C70.90 specimens, which may have led to more energy absorption. The effect of tufting may therefore be twofold: strengthen the facesheet/core interface and preventing premature delaminations in-between the facesheet plies. This is similar to the finding of Stapleton and Adams [14], who used biaxial Kevlar® stitching to improve the SEA crushing response of woven CFRP/polyurethane sandwiches by 224.5%. In addition, the failure mechanisms within the tufts are the topic of on-going research [25]. Identifying the individual contributions of the core, facesheets and fracture of the tufting thread may help better understand the crushing process.

4. Conclusions

The edgewise crushing response of foam core sandwich panels was investigated in this study by considering brittle and ductile core, facesheet lay-up, and through-thickness reinforcement by tufting. The most significant improvement in edgewise crushing response was obtained by tufting the sandwich panels with aramid fibre threads. Both specific energy absorption (SEA) and crush force efficiency (CFE) increased by an average of 78%, and 129%, respectively. The tufted specimens showed more localized and stable fracture of the facesheets, leading to a higher sustained crushing load and as a result better absorbing more energy than their untufted counterparts.

The non-tufted sandwich structure failure was dominated by facesheet/core disbonding and delaminations within the facesheet plies. The failure mechanism of the untufted structures was governed by the foam core and skin thickness. A ductile core stabilised the facesheets, allowing energy absorption through ply/ply delamination, whereas a brittle core encouraged facesheet/core disbonding. Accordingly, thicker facesheets with more ply interfaces absorbed more energy, however weak facesheet/core interfaces inhibited fracture of the actual carbon fibres, which is the main energy absorption mechanism activated by tufting the facesheet to the core.

Overall, through-thickness reinforcement by tufting showed the ability to stabilise and tailor the crushing response of fibre reinforced sandwich structures. This may be used to exploit new load-paths in crash structures, and as a result, increase the crashworthiness of composite structures in a larger variety of load cases.

Acknowledgements

The authors would like to acknowledge BMW Group for their financial support towards this project, providing the testing facilities and the materials. This work is further supported with the help and expertise provided by the Delft University of Technology and by the UK Engineering and Physical Sciences Research Council (EPSRC) under the Impact Acceleration Award scheme at the University of Bristol (EP/K503824/1). The UK National Composites Centre is acknowledged for granting access to the tufting equipment. Finally, we would like to thank Mr. Greissl and Mr. Palmer for help conducting the tests.

Access to supporting data may be requested from the corresponding author, which due to commercial contracts in place, will be subject to consent being granted from the original project participants.

References

[1] Carruthers JJ. Energy absorption capability and crashworthiness of composite material structures: a review. Appl Mech Rev 1998;51(10):635–49.
[2] Johnson W. The elements of crashworthiness: scope and actuality. Proc Inst Mech Eng Part D J Automob Eng 1990;204(4):255–73.
[3] Lukaszewicz DH-J A. Automotive composite structures for crashworthiness. In: Advanced composite materials for automotive applications. John Wiley & Sons Ltd; 2013. p. 99–127.
[4] Hull D. A unified approach to progressive crushing of fibre-reinforced composite tubes. Compos Sci Technol 1991;40(4):377–421.
[5] Farley GL, Jones RM. Crushing characteristics of continuous fiber-reinforced composite tubes. J Compos Mater 1992;26(1):37–50.
[6] Warrior NA, Turner TA, Robitaille F, Rudd CD. The effect of interlaminar toughening strategies on the energy absorption of composite tubes. Compos Part A Appl Sci Manuf 2004;35(4):431–7.
[7] Hamada H, Ramakrishna S, Nakamura M, Maekawa Z, Hull D. Progressive crushing behaviour of glass/epoxy composite tubes with different surface treatment. Compos Interfaces 1994;2(2):127–42.
[8] Thornton PH, Jeryant RA. Crash energy management in composite automotive structures. Int J Impact Eng 1988;7(2):167–80.
[9] Tao WH, Robertson RE, Thornton PH. Effects of material properties and crush conditions on the crush energy absorption of fiber composite rods. Compos Sci Technol 1993;47(4):405–18.
[10] Farley GL. Energy absorption of composite materials. J Compos Mater 1983;17(3):267–79.
[11] Mamalis AG, Manolakos DE, Ioannidis MB, Papapostolou DP. On the crushing response of composite sandwich panels subjected to edgewise compression: experimental. Compos Struct 2005;71(2):246–57.
[12] Velecela O, Found MS, Soutis C. Crushing energy absorption of GFRP sandwich panels and corresponding monolithic laminates. Compos Part A Appl Sci Manuf 2007;38(4):1149–58.
[13] Stapleton SE, Adams DO. Crush initiators for increased energy absorption in composite sandwich structures. J Sandw Struct Mater 2008;10(4):331–54.
[14] Stapleton SE, Adams DO. Structural enhancements for increased energy absorption in composite sandwich structures. J Sandw Struct Mater 2011;13(2):137–58.
[15] Mouritz AP, Bannister MK, Falzon PJ, Leong KH. Review of applications for advanced three-dimensional fibre textile composites. Compos Part A Appl Sci Manuf 1999;30(12):1445–61.
[16] Potluri P, Kusak E, Reddy TY. Novel stitch-bonded sandwich composite structures. Compos Struct 2003;59(2):251–9.
[17] Dell'Anno G, Treiber JWG, Partridge IK. Manufacturing of composite parts reinforced through-thickness by tufting. Robot Comput Integr Manuf 2016;37:262–72.
[18] Henao A, Carrera M, Miravete A, Castejón L. Mechanical performance of through-thickness tufted sandwich structures. Compos Struct 2010;92(9):2052–9.
[19] SGL Group, SIGRAFIL Continuous Carbon Fiber Tow, 2016. [Online]. Available: <www.sglgroup.com>. [Accessed: 30-Oct-2016].
[20] 3A Composites, Airex C70 Data sheet, vol. 2011, 2011.
[21] Evonik Industries AG, Rohacell IG/IG-F Technical Information, 2014.
[22] Velecela O, Soutis C. Prediction of crushing morphology of GRP composite sandwich panels under edgewise compression. Compos Part B Eng 2007;38(7–8):914–23.
[23] Society of Automotive Engineers, Instrumentation for impact tests – Part 1 – Electronic instrumentation – SAE J211/1. p. 34.344–34.35,; 1995.
[24] Mamalis AG, Manolakos DE, Demosthenous GA, Ioannidis B. Crashworthiness of composite thin-walled structures. Taylor & Francis; 1998.
[25] Hartley JW, Tse G, Kratz J, Ward C, Partride I. Column interaction in tufted sandwich structures under edgewise loading. In: ECCM17 – 17th European conference on composite materials.